ORIGINAL ARTICLE

Shear thickening fluids in cork composites for impact mitigation: the role of fumed silica concentration

L. Oliveira[1] · G. F. Serra[1,2] · S. Gürgen[3] · R. M. Novais[4] · R. J. Alves de Sousa[1,2] · F. A. O. Fernandes[1,2]

© The Author(s) 2024

Abstract

Cork composites have shown excellent potential in impact mitigating systems. Their sustainability greatly surpasses the currently used solutions. In addition, recent advances in developing cork composites with shear thickening fluids (STFs) have demonstrated exciting results for impact mitigation. This study explores different STF formulations based on polyethylene glycol (PEG), with a molecular weight of 400 g/mol, and SiO_2 particles, investigating their application in layered cork composites for impact mitigation. Different STF formulations are investigated by processing suspensions with different fumed silica concentrations ranging from 10 to 60 wt.%. Using a cone–plate configuration, rheological measurements were conducted on these suspensions, which were then employed as an interfacial layer in agglomerated cork composite layered structures. These hybrid composites were then subjected to 20 J impact tests. PEG 400 exhibited fluid final states for silica concentrations up to 30 wt.% and crystallised at higher concentrations. Based on the results, STF within cork layers was positive regarding impact force reduction, drawing insights for future application of STF suspensions in cork composites for impact mitigation.

Graphical abstract
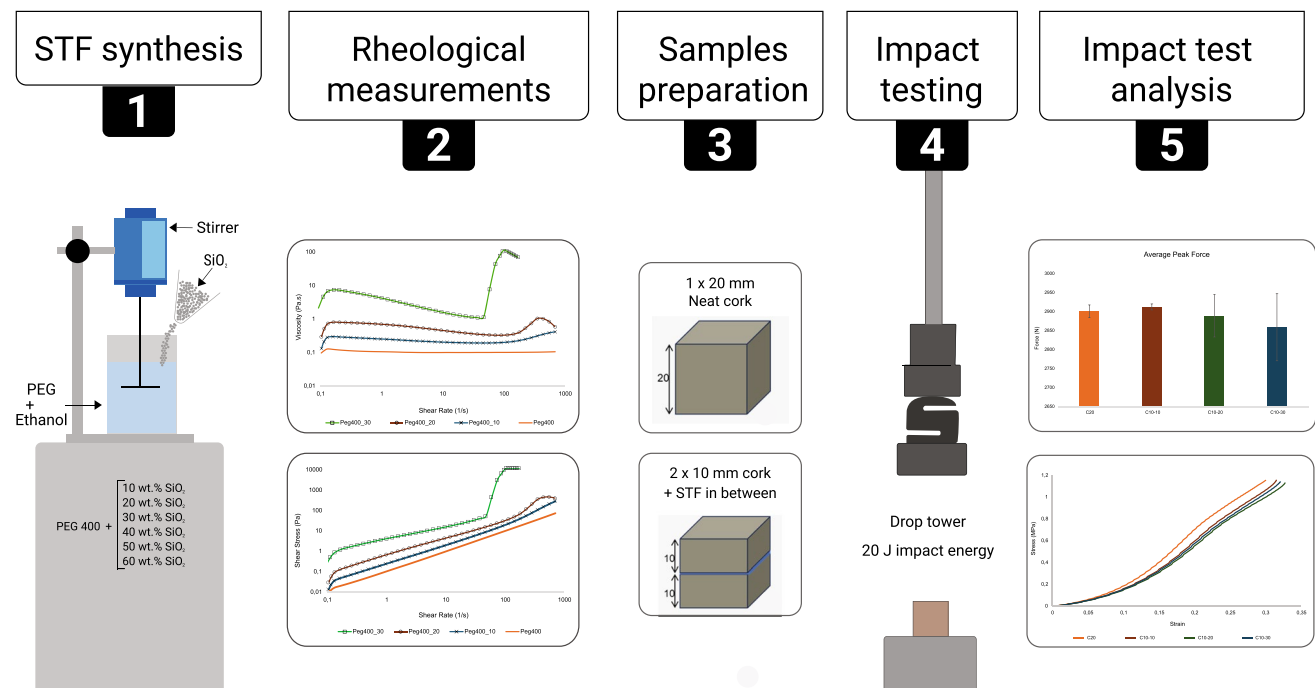
Extended author information available on the last page of the article

1 Introduction

Fluids can be defined by their viscosity, which measures a fluid's resistance to shear flow. In Newtonian fluids, viscosity remains independent of the shear strain rate, while in non-Newtonian fluids, viscosity varies according to the applied shear rate [1]. Shear thickening fluids (STFs) fall into the category of non-Newtonian fluid, transitioning from a liquid state at low shear rates to a solid-like state at higher shear rates, which is attributed to a rapid increase in viscosity [2].

Barnes [3] posited that although challenging to measure consistently, shear thickening behaviour is inherent in most suspensions. The term "suspension" refers to a biphasic system where a solid phase is present in a continuous (fluid) phase [4]. The rheological behaviour of fluids depends on various factors, including suspension stability, the viscosity of the continuous phase, and particle size distribution, among others. The hydroclustering and friction contact theories explain the shear thickening phenomenon. The hydroclustering theory suggests that hydrodynamic interactions on the dispersed particles grow stronger upon increasing the shear rate in the suspension. Hence, particles get closer to each other, forming particle clusters, namely hydroclusters in the suspension. Hydroclusters act as barriers by hindering the fluid from flowing, ultimately leading to a viscosity increase in the suspension. As the shear rate further increases, interparticle distances reduce to such an extent that particles physically contact each other. Consequently, based on the friction contact theory, the contacted microstructure extends inside the suspension by withstanding the developed stresses during the shear thickening phenomenon. To sum up, shear thickening onset is triggered by the hydroclustering, while further viscosity increase is driven by the particle contacts in the suspension [5].

This shear thickening behaviour of fluids aroused the curiosity of various industry sectors, and their use can be seen in a wide range of applications that go from aircraft to automobiles and bullet-proof vests. Its use has mainly been investigated for protective applications due to its capacity to absorb energy in high-velocity impacts. Using textiles impregnated with STF has proven to be very effective for protection as the fluid increases inter-yarn friction in the fabrics, leading to higher levels of energy absorption [6, 7]. Lu et al. [8] incorporated STFs into warp-knitted spacer fabrics (WKSF) to explore the fabric's behaviour under quasi-static compression and low-velocity impact loadings, with results suggesting that these STF/WKSF systems have the potential to serve as damping materials for personal protection. Similarly, Gürgen and Kuşhan [9] studied the behaviour of high-performance fabrics impregnated with STFs enhanced with SiC particles in a drop tower against spike and knife threats, concluding that the fluid enhanced the overall stab resistance of the fabric.

Composite structures employing STF have also proven efficient, providing enhanced protection and reduced weight. For instance, Tan et al. [10] examined sandwich structures comprising pure aluminium sheets with STFs. During impact tests conducted with a gas gun unit, steel projectiles were fired at speeds ranging from 30 to 120 m/s. The results revealed that the shear thickening mechanism of STFs becomes more pronounced at higher striking velocities. Another type of efficient composite is incorporating STF into the matrix of a fibre-reinforced polymer (FRP) [11, 12]. With the incorporation of non-Newtonian fluids into carbon fibre-reinforced polymer composites (CFRP), for instance, it is possible to further enhance the material's impact resistance, with the energy absorption level increasing by 45% [13].

Studies have also started investigating combining STF with more sustainable materials, such as cork. Cork is a cellular material that is 100% natural, and it can be described as a homogeneous tissue of thin wall cells arranged without intercellular space [14]. The natural cork is usually used to produce wine stoppers, and the waste generated by it is used to make agglomerated cork by mixing the cork granules with a binder (polyurethane, melaminic or phenolic resins) and then compression moulded in a temperature-aided process. This by-product of wine stoppers has excellent potential for crashworthiness applications [10, 15, 16], and combining it with STF demonstrated that it yielded some excellent results in different ways.

Gürgen and Alves de Sousa [17] investigated the rheological impact of adding cork granules (0.5–1.0 mm) to two shear thickening suspensions—one natural with water and cornstarch and another with silica and polyethylene glycol (PEG). The authors found that cork granules enhanced STF rheology, presenting a promising eco-friendly additive. Silica-based mixtures exhibited improved stability at higher shear rates due to harder silica particles compared to cornstarch. However, the deformable nature of cork diminished shear thickening properties with an increase in the number of cork grains in the mixtures.

Serra et al. [18] evaluated different configurations, including cork-STF impregnated fabric, bulk STF as an interlaying agent between cork samples, encapsulated STF between cork and thermoplastic polyurethane (TPU), and cork-STF filled polymers, by subjecting samples to low-energy (20 J) and high-energy (100 J) drop impact tests using a 20 kg flat impactor mass. STF performed better in bulk form under high-energy impacts, reducing peak acceleration by 8.50% and providing smoother deceleration. In another study, Gürgen et al. [19] investigated a multi-layered structure comprising cork laminates with STF, comparing it to neat cork laminates. Impact tests at 5 J, 10 J, and 15 J were conducted on 20-mm-thick composite structures varying cork plank thicknesses (2 mm, 5 mm, 10 mm, and 20 mm). Neat cork laminates had no additional material, while other samples included 1 g of STF at each interface. The best design achieved a 36% maximum force reduction with ten layers at 5 J. The study indicated that the multi-layered structure was more effective for lower energy impacts but showed limitations for higher energy impacts of 10 J and 15 J. Despite this, the composite exhibited promising properties for damping, shock absorption, and crashworthiness.

From the literature, STF provides excellent anti-impact properties due to its adaptive rheology. On the other hand, cork composites have been widely used in impact mitigation structures to benefit from their low-density and impact resistance and sustainable and eco-friendly advantages. Therefore, combining these two materials is interesting for eco-structures designed for impact mitigation. By combining these two anti-impact materials, this work investigates how cork-STF sandwich structures perform under dynamic impacts. However, in contrast to the previous study [19], the focus is exploring different STF formulations based on PEG and silica nanoparticles and validating their application in cork composite layered structures. Specifically, these STF formulations are based on PEG with a molecular weight of 400 g/mol mixed with fumed silica particles in ratios ranging from 10 to 60 wt.%. Shear thickening behaviour was investigated through rheological measurements under increasing shear rates, and both the viscosity and developed shear stresses were investigated. Additionally, sandwich structures were manufactured with the STF acting as an interlaying agent between two layers of agglomerated cork sheets and subjected to impacts of 20 J using a drop tower to explore the effectiveness of the structures' energy absorption capacity.

2 Materials and methods

2.1 Materials used in the experiments

In this study, composites composed of agglomerated cork and various formulations of STFs underwent dynamic impact tests using a drop tower. The agglomerated cork is a compound with a 170 kg/m^3 density, which Unicor supplied in the form of 10- and 20-mm-thick boards. More properties are presented in Table 1.

For the STF synthesis, PEG with a molecular weight of 400 g/mol from Thermo Scientific Acros was employed as the continuous phase. The properties of the PEG are given in Table 2. Fumed silica (SiO$_2$) nanoparticles with a specific surface area of 200 ± 25 m^2/g were supplied by Merck. The properties of the fumed silica particles are given in Table 3. Also, absolute ethanol (99.5% vol.) from Aga was employed.

Besides being cost-effective and chemically stable, STFs based on SiO$_2$ and PEG can withstand higher shear rates due to the inherently thick texture of PEG, so higher forces can be overcome during the shear thickening process.

2.2 STF synthesis

PEG is chosen as the continuous phase due to its low volatility, thermal stability and non-toxic properties [2]. However, there is no precise pattern or procedure in the literature concerning the experimental methodology and conditions, making it harder to compare the influence of different factors on the rheological behaviour of the suspensions [2, 19–23].

The T18 brushless digital Ultra-Turrax, a high-performance disperser from Ika, was employed to homogenate the silica nanoparticles in the PEG. This equipment made it possible to mix the two elements homogeneously. The suspensions were subjected to a 2 h dispersing process at 15,000 rpm for six different silica loadings from 10 to

Table 1 Agglomerated cork properties (ISO 7322)

Density [kg.m^{-3}]	Tensile strength [kPa]	Recovery [%]	Dimensional stability [%]
170	650	75	0.5

Table 2 Properties of polyethylene glycol

Properties	Molecular weight [g/mol]	Density [kg.m^{-3}]	Flash temperature [°C]	Melting point [°C]	Viscosity @ 20 °C [mPa.s]
PEG 400	400	1,128	235	4–8	110–125

Table 3 Properties of fumed silica nanoparticles (SiO$_2$)

Molecular weight [g/mol]	Melting point [°C]	Density [kg.m^{-3}]	Water solubility [g/l] @ 37 °C	Particle size [mm]	Spec. surface area [m^2/g]
60.08	1,713	2,560	0.076	< 0.5	200 ± 25

60wt.%. Ethanol absolute was also used to disperse the SiO_2 particles quickly by diluting the suspension. In each formulation, approximately one-third of ethanol was used for the quantity of PEG, which, in the end, is evaporated to achieve the desired suspension.

The initial step involved blending ethanol with PEG and adding silica until the desired concentration was attained (illustrated in Fig. 1). The fumed silica was added gradually to prevent agglomeration, as recommended in the literature [24, 25]. Due to the elevated viscosity of formulations with silica concentrations equal to and higher than 40 wt.%, these were subjected to a hot plate at 50 °C to expedite ethanol evaporation.

After the STF preparations, STFs based on 10 wt.%, 20 wt.%, and 30 wt.% of SiO_2 exhibited a fluid final state (Fig. 2). However, for higher SiO_2 concentrations, the STFs crystallised, as shown in Fig. 3. Therefore, there are no rheological results for STFs with SiO_2 concentrations higher than 30 wt.%.

2.3 Rheological measurements

Non-Newtonian rheology of the developed STFs was investigated in a Kinexus Rheometer (Kinexus Pro +, Netzsch, Selb, Germany) by using a cone–plate configuration with a contact angle of 4°, a 40-mm radius, and a gap of 150 μm between cone and plate (Fig. 4). This equipment is linked to rSpace software, enabling real-time monitoring of rheological tests. The temperature for each test was controlled, with all tests conducted at 25 °C. Each STF underwent shearing from 0 to 1000 s^{-1} shear rate.

To study the rheological properties of STFs, several key parameters were analysed: initial viscosity (η_0), critical shear rate ($\dot{\gamma}_C$), critical viscosity (η_C), maximum shear rate ($\dot{\gamma}_{max}$), and maximum viscosity (η_{max}). The thickening ratio (TR) and the thickening period (TP) were also analysed based on Eqs. 1 and 2, respectively.

$$TR = \frac{\eta_{max}}{\eta_C} \tag{1}$$

$$TP = \dot{\gamma}_{max} - \dot{\gamma}_C \tag{2}$$

2.4 Impact testing of cork-STF composite structures

Two different types of samples were created: (i) a 20-mm-thick cork sample (Fig. 5a); (ii) a sandwich configuration made with two 10-mm cork samples with 1 g of STF spread on the interface (Fig. 5b). Their designations are represented in Table 4. All the samples have the following dimensions at the final state: $50 \times 50 \times 20$ mm^3. Prior to conducting the impact tests, all samples underwent weighing, and the mass values are detailed in Table 5.

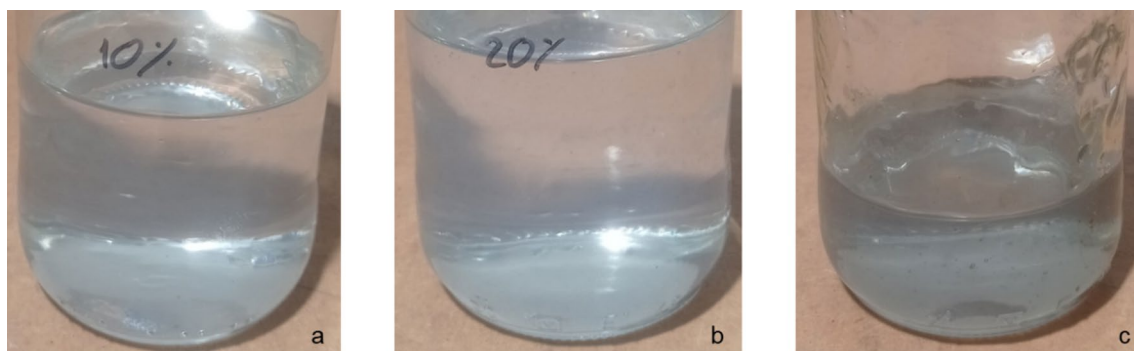**Fig. 1** Representation of the STF synthesis process

Fig. 2 Fluid final state of PEG 400 with a concentration of SiO_2 of: **a** 10 wt.%; **b** 20 wt.%; **c** 30 wt.%
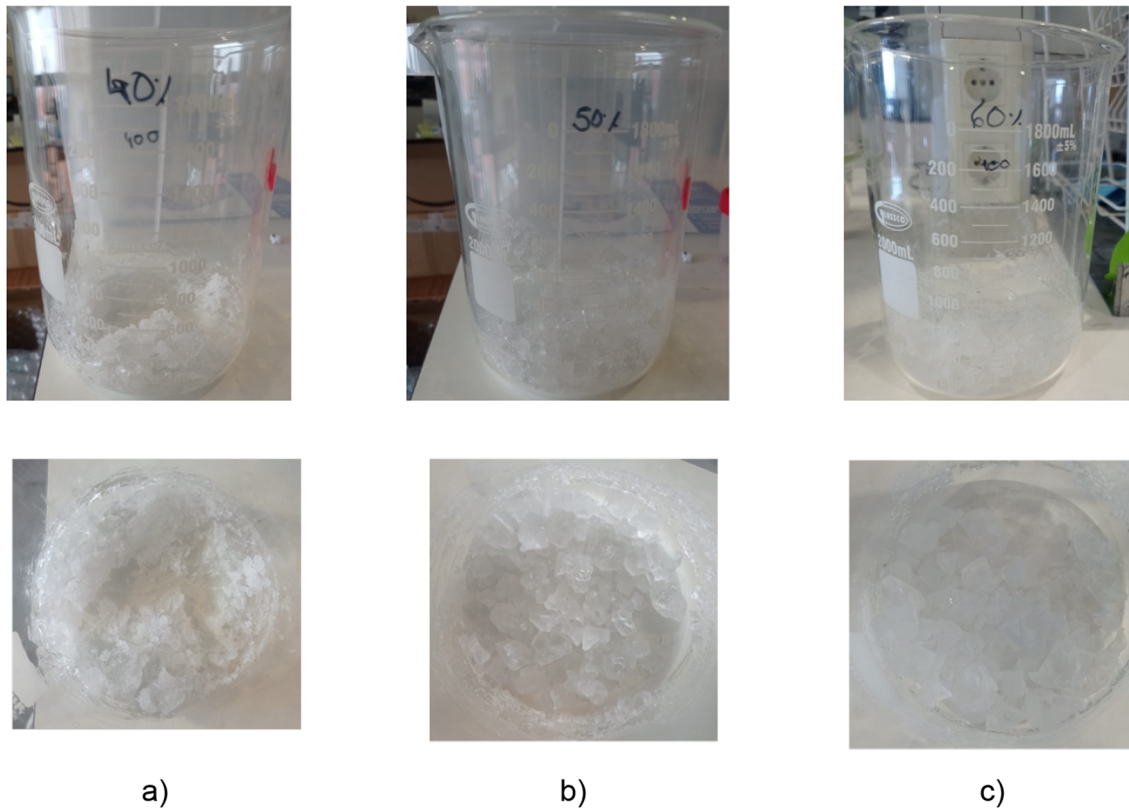
Fig. 3 Crystallised STFs due to excessive silica contents; **a** 40 wt.%; **b** 50 wt.%; **c** 60 wt.%
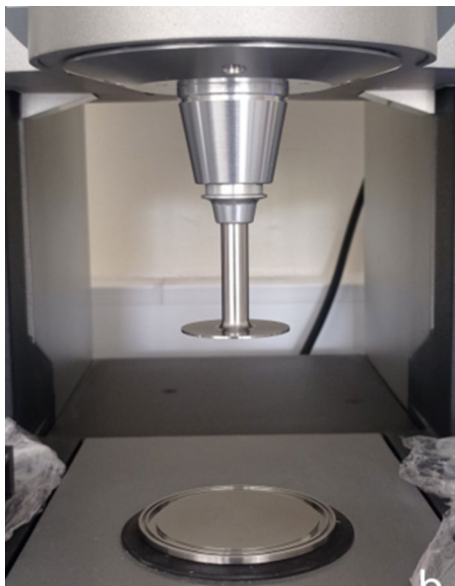

Fig. 4 Kinexus rheometer (Kinexus Pro +, Netzsch, Selb, Germany): Cone–plate configuration
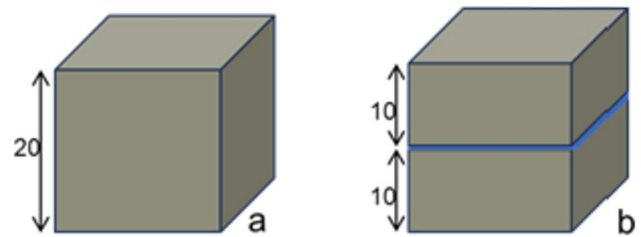

Fig. 5 Schematic representation of samples: **a** 20 mm of thickness (sample code: C20); **b** 10 mm of thickness with 1 g of STF at the interface (sample codes: C10-XX—see Table 4)

Table 4 Cork-STF samples designation

Sample	Code
Cork with 20 mm	C20
Two cork layers with 10 mm and PEG400 with 10 wt.% of SiO_2	C10-10
Two cork layers with 10 mm and PEG400 with 20 wt.% of SiO_2	C10-20
Two cork layers with 10 mm and PEG400 with 30 wt.% of SiO_2	C10-30

The impact tests were performed in a drop tower. The stainless steel impactor has a diameter of 130 mm and weighs 20 kg (Fig. 6). The impact force is measured thanks

Table 5 Average mass of the samples

Sample type	mass (g)
C20	12.00 ± 0.10
C10 (without STF)	12.78 ± 0.13
STF	1.04 ± 0.03
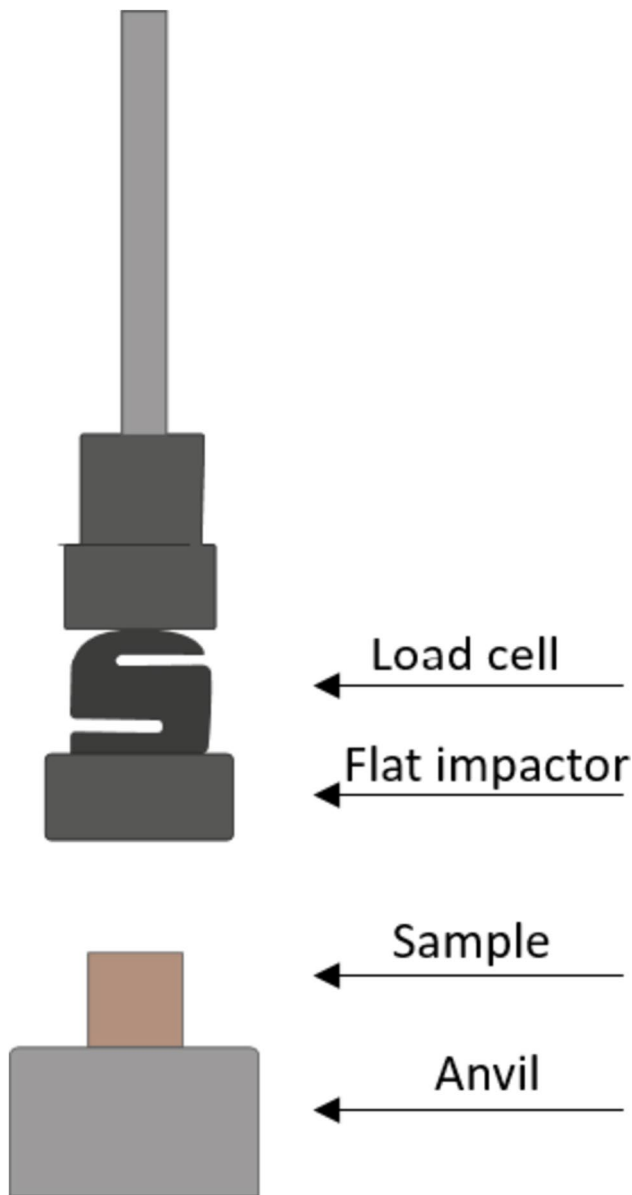
Fig. 6 Representation of the impact test setup

to a load cell in the impactor setup. All the samples were centred on the steel anvil. The impact corresponds to a uniaxial guided mass, gravitically falling from a height of 103 mm to attain an impact energy of 20 J.

3 Results and discussion

3.1 STF synthesis and rheological measurements

In Fig. 7, the viscosity shear rate curves for all STFs are depicted. Since SiO_2 concentrations higher than 30 wt.% induce a crystallisation phenomenon, rheological tests were exclusively conducted on mixtures ranging from 10 to 30 wt.%. It is evident that PEG, serving as the continuous phase of the STF, maintains a constant viscosity with an increasing shear rate. However, adding silica particles transforms the Newtonian behaviour of PEG into a non-Newtonian one.

It is possible to see that silica inclusion increases the initial viscosity of the continuous phase. This is simply due to the increased density in the suspension that directly leads to an increase in the initial viscosity. By introducing solid particles in the liquid medium, interparticle adhesion produces a thicker texture in the fluid [26]. As shown in Fig. 7, this effect gets stronger by including more solid particles in the suspension.

According to the hydroclustering theory, the onset of shear thickening is due to the hydrodynamic interactions between the silica particles and liquid medium. Hydrodynamic forces on the silica particles gradually increase upon shearing the mixtures, thereby overcoming the interparticle repulsive forces. The particles come closer to each other, forming hydroclusters this way. Due to the hydroclusters, the fluid is hindered from flowing by showing a viscosity jump in the rheological curves. Considering the sample with 10 wt.% silica loading, the shear thickening phenomenon is frail, showing a slight viscosity increase beyond the shear rate of 100 s^{-1}. This can be associated with insufficient silica particles to develop strong hydrodynamic forces. Hence, poor hydroclustering is observed, requiring relatively high shear rates to extend the suspension. However, shear thickening grows stronger by including more silica particles in the samples. At the silica concentration of 20 wt.%, shear thickening initiates at an earlier shear rate while showing a higher peak viscosity. Further at 30 wt.%, hydroclustering is triggered at a much lower shear rate, sufficient to elevate the hydrodynamic forces due to the increased number of silica particles. In denser suspensions, interparticle distances reduce, forming larger hydroclusters at lower shear rates [27]. As a result, viscosity shows a sharper jump with a higher peak point in viscosity.

Figure 8 shows the shear stress profiles in the suspensions. The chart shows that suspensions bear higher stresses as silica concentration increases in the medium. This is related to the load-bearing capacity of the suspensions, which grows with the addition of more silica

Fig. 7 Viscosity shear rate curves of STFs
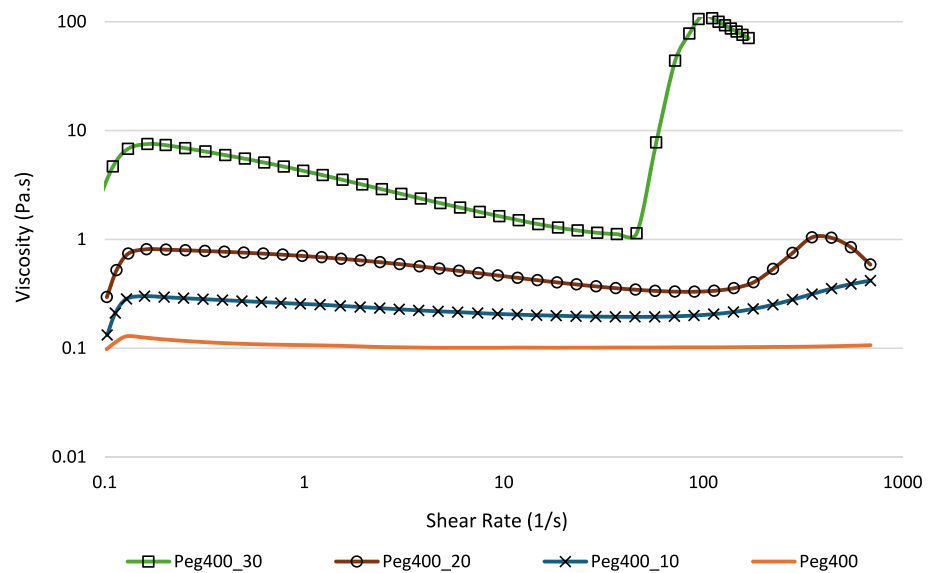
Fig. 8 Shear stress–shear rate curves of STFs
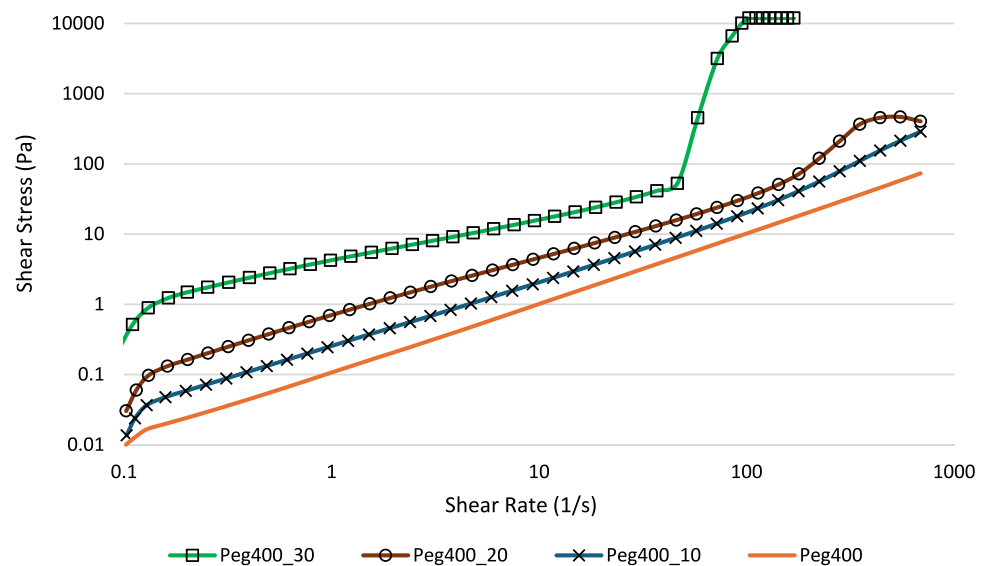
particles in the samples. Hydroclustering triggers the shear thickening onset, and particle contacts occur at higher shear rates, where strong shear thickening prevails in the suspension.

Silica particles are hard components that can resist elevated stresses without failure during the shear thickening process. For this reason, a higher amount of silica particles leads to the extension of contacted particle networks in the suspension. Hence, higher viscosity jumps can be attained without failure due to the higher stress-bearing capabilities of elongated particle networks. Beyond the peak viscosity points, the particle networks cannot bear the developed stresses in the suspensions. For this reason, the suspensions show an immediate viscosity drop after reaching the peak viscosities. In this phase, contacted particle networks show

a structural breakdown, and therefore, the elongated large particle extensions are broken into small particle branches. In some cases, particles show plastic deformations such as crashes if the developed stresses exceed the allowable strength of the particle materials. For example, cornstarch-based suspensions are more likely to involve these deformations during the shear thickening process due to the very soft nature of cornstarch particles [17].

Table 6 presents the main rheological parameters for the STFs. From these results, initial viscosity shows an increasing trend by including more silica particles in the suspensions. As previously explained, particle addition increases the suspension density, which leads to an increase in viscosity. On the other hand, the critical shear rate reduces as silica concentration increases in the

Table 6 Characteristic parameters of STFs

SiO$_2$ in STF (wt.%)	η_0 (Pa.s)	$\dot{\gamma}_c$ (1/s)	η_C (Pa.s)	$\dot{\gamma}_{max}$ (1/s)	η_{max} (Pa.s)	TR	TP (1/s)
10	0.132	114	0.21	689.2	0.48	2.03	576.2
20	0.295	113.6	0.34	351.3	1.04	3.10	237.7
30	2.162	46.4	1.14	102.7	116.2	102.20	56.3

samples. This means that shear thickening initiates at lower shear rates by the effect of increased particle loadings. Suspensions show elevated hydrodynamic forces acting on the particles at high concentrations, so hydroclustering occurs at lower shear rates.

Critical viscosity (viscosity at the critical shear rate) systematically increases with the silica loading. It is the exact mechanism with the initial viscosity increase. Because the particle amount increases in the suspension and, denser textures increase viscosity at a critical shear rate. Although the rheological measurements were conducted for the shear rate interval from 0 to 1000 s^{-1}, the samples could not show stable characteristics till the shear rate of 1000 s^{-1}. Hence, the tests were terminated at earlier shear rates, the maximum shear rates for the samples.

From the results, the maximum shear rate is reduced by increasing silica concentration in the samples. At low particle loadings, suspensions require higher shear rates to elevate the hydrodynamic forces to the shear thickening onset. However, lower shear rates are sufficient to develop the required levels of hydrodynamic forces due to the increased number of silica particles. In the same way, the shear thickening process is completed at lower shear rates, and the suspensions lose their stabilities due to the breakdown of particle contacts beyond the peak viscosities. For this reason, the maximum shear rate gradually reduces by including more particles in the samples.

Maximum viscosity is one of the main parameters describing the shear thickening behaviour in the suspensions. The results show that maximum viscosity increases with SiO$_2$ particle concentration in the samples. This is attributed to the extension of contacted microstructures with more silica particles in the suspensions. According to Bossis et al. [28], hydrodynamic stresses are proportional to the dimension of contacted particle elongations, which means that the shear thickening process gets stronger, and consequently, higher viscosities can be attained as the particle contacts grow larger due to the increased number of silica particles in the samples.

The thickening ratio is another important metric, showing the intensity of shear thickening properties in the suspensions. The results show that adding more silica particles to the samples increases the thickening ratio. There is a drastic jump in the thickening ratio, from 2.03 to 102.20, when the silica loading increases from 10 to 30 wt.%. It can be

mentioned that the increase in the silica phase considerably enhances shear thickening behaviour.

Larger thickening periods are associated with poor shear thickening properties [29, 30]. This is associated with the lower hydrodynamic interactions and insufficient formation of contacted microstructure that delay the completion of shear thickening over a wider period. The results obtained in this work reveal that the thickening period was reduced by increasing the silica content. Hence, it can be stated that the shear thickening process is completed in shorter periods for the suspensions with higher particle loadings due to their strong shear thickening behaviour.

3.2 Impact tests

Figure 9 compares the average peak forces obtained for each sample. As shown in the graph, sample C20, the cork block without STF, shows an average peak force of 2901.1 N. On the other hand, C10 samples incorporating STF have the average peak forces of 2912.4 N, 2888.9 N and 2858.7 N for the silica loadings of 10 wt.%, 20 wt.%, and 30 wt.%, respectively. Despite the higher peak force with C10-10 compared to C20, samples C10-20 and C10-30 show lower peak forces than sample C20 in the drop tests.

It can be mentioned that STFs with 20 wt.% and 30 wt.% silica concentrations improve the impact mitigation behaviour of the cork structures. In C20, the impact force is accumulated only on the impact point. Hence, the impact absorption of the cork structure cannot be benefitted to a great extent. However, the STFs at the interface of the cork layers exhibit an increase in viscosity upon impact. The shear thickening effect in the samples consumes a part of the impact energy.

Despite the additional impact absorbing effect of STF, sample C10-10 falls behind the sample C20. Recalling Fig. 7, this can be attributed to the frail shear thickening behaviour of the suspension with 10 wt.% silica loading. The STF in C10-10 behaves like a Newtonian fluid, showing almost no shear thickening mechanism. Thus, the cork structure cannot take advantage of the viscosity increase in this sample.

Table 7 shows the impact durations for each sample. Despite the minimal differences, STF applications extend the impact process over a larger time period. Therefore, the impact is suppressed in longer time intervals by the effect of

Fig. 9 Comparison between the average peak force registered for samples C20, C10-10, C10-20 and C10-30 with the respective standard deviation
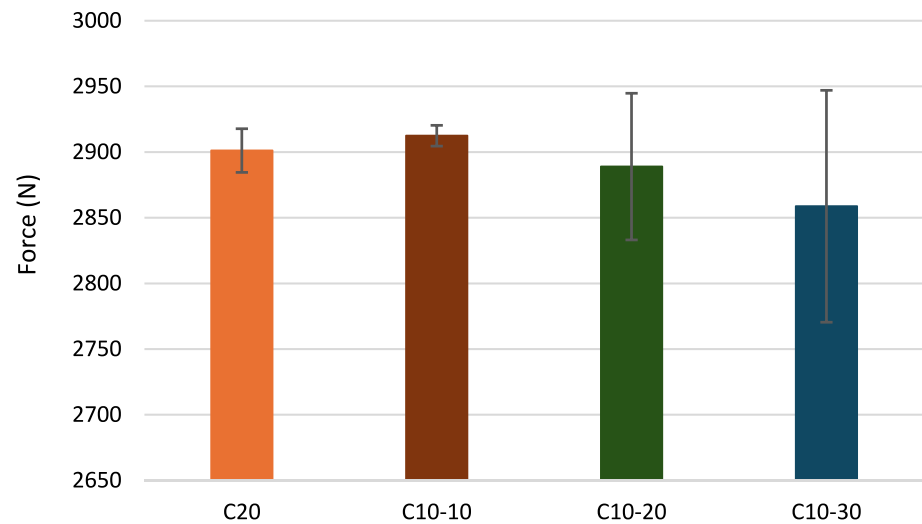

Table 7 Duration of impacts

	C20	C10-10	C10-20	C10-30
Duration of impact (ms)	28	29.12	29.96	28.36

STFs. It is also important to note that STFs at the cork layer interfaces are not surrounded, so there is no restriction at the boundaries. For this reason, some STF splashing from the samples occurs, leading to a performance loss in the shear thickening effect. This aligns with the findings of Serra et al. [18] for similar multi-layer configurations of cork-STF samples subjected to the same impact conditions.

Configurations with unrestrained STF seem to perform less effectively under both low- and high-energy impacts, possibly due to the lack of boundaries allowing the fluid to escape upon impact, reducing its capacity to dissipate the impact energy. This issue was also recently raised and investigated by Sheikhi et al. [31], where benefits from encapsulating STF were highlighted.

Figure 8 depicts the most representative stress–strain curve from each type of sample. From observing the stress–strain plots in Fig. 10, a clear pattern emerges, with all the samples exhibiting the same behaviour, evidently governed by cork. Although the samples have the same size, in order to make the data from this study comparable for future reference, the strain energy density (strain energy per unit of volume) was determined. The strain energy density corresponds to the area under the stress–strain curve. Table 8 compares the average strain energy density obtained for each sample type subjected to the impact tests. Overall, the values obtained for each

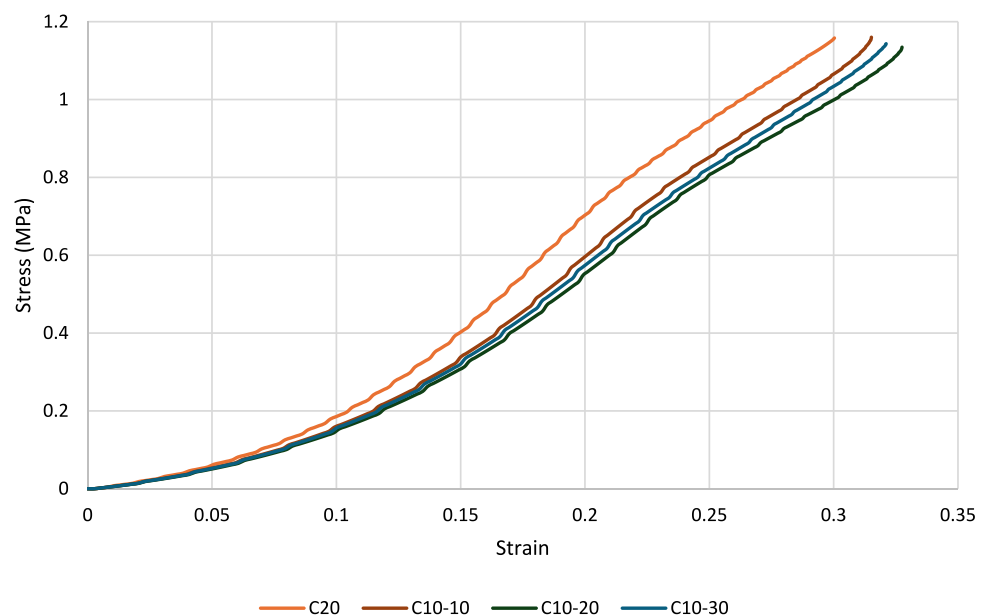**Fig. 10** Representative stress–strain curves from the impact tests

Table 8 Average strain energy density

	C20	C10-10	C10-20	C10-30
Strain energy density (kJ/m^3)	145.09	144.24	148.43	146.05

type are similar. Nevertheless, the samples with 20 wt.% and 30 wt.% SiO$_2$ loadings present slightly higher values. These samples exhibit lower peak forces corresponding to the strain energy densities.

Overall, the STF reduced the impact force compared to the neat cork structure for higher silica concentrations of 20 wt.% and 30 wt.%. However, at the silica amount of 10 wt.%, the structure cannot benefit from the shear thickening effect since the viscosity jump is reasonably limited in this particular formulation. Moreover, the amount of fluid used as an interlayer agent in this study is relatively low, which can also limit the benefits of shear thickening in impact response. As Gürgen et al. [19] reported in a study with similar cork-STF sandwich structures, samples with only one layer of STF between cork sheets performed worse than neat cork samples for higher levels of impact energies (15 J). Conversely, samples with more layers (but the same overall structure thickness), consisting of ten layers of cork and nine layers of STF in between, which consequently increased the weight fraction of the fluid regarding the composite, performed better for all energy levels, resulting in a reduction in maximum impact forces ranging from about 8% to almost 40%.

This exploratory work suggests the potential of using STF to enhance the impact performance of composites, particularly those based on cork. New configurations can be explored based on this work. For instance, restricting the STF from freely flowing upon impact can potentially enhance the composite's performance under impact. Also, tuning the STF / structure weight ratio can significantly benefit the performance in terms of crashworthiness [19]. As rheological results partially demonstrate and other studies indicate [9, 30, 32–34], good shear thickening properties can be obtained using at least 20 wt.% of silica (depending on the continuous phase). Overall, this preliminary study made it possible to draw insights for future studies on these applications, exploring alternative STF formulations, composite designs, and different methods.

4 Conclusions

This study developed cork composite structures with STF formulations, focusing on the influence of silica particle concentrations. The STF application between cork layers to enhance impact performance was investigated. In summary, this study concludes that:

- SiO$_2$ particle concentrations up to 30 wt.% in PEG demonstrated effective shear thickening.
- The suspension with 30 wt.% silica demonstrated excellent performance, exhibiting a high thickening ratio, a good thickening period, favourable viscosity and critical shear rate levels.
- SiO$_2$ particle concentrations within 40–60 wt.% exhibited crystallisation issues.
- Low-energy impact tests on the cork-STF composite structures revealed that increasing silica concentration in the STF led to lower peak forces, indicating improved impact mitigation.

The present work suggests the potential of STF to enhance impact performance in cork-based composites, opening avenues for future exploration in alternative formulations and composite designs. Cork composites present interesting properties for several applications, such as damping and shock absorption. This preliminary work makes it possible to conclude that the STF can reduce the impact force and increase the energy absorption of cork composites. Therefore, cork-STF composites present interesting properties for damping and shock absorption applications.

Declarations

References

1. K. Van Canneyt, P. Verdonck, 10.02 - Mechanics of Biofluids in Living Body, in: A. Brahme (Ed.), Comprehensive Biomedical Physics, Elsevier, Oxford, 2014. 39–53. https://doi.org/10.1016/B978-0-444-53632-7.01003-0.

2. Kang TJ, Kim CY, Hong KH. Rheological behavior of concentrated silica suspension and its application to soft armor. J Appl Polym Sci. 2012;124:1534–41. https://doi.org/10.1002/app.34843.

3. Barnes - 2000 - A handbook of elementary rheology.pdf, (n.d.). https://ia601206.us.archive.org/4/items/HandbookOfRheology/Handbook_of_Rheology.pdf (accessed January 5, 2024).

4. Ozel BG, Orum A, Yildiz M, Menceloglu YZ. Experimental study on the rheology of anisotropic, flocculated and low volume fraction colloids. Korea-Aust Rheol J. 2014;26:105–16. https://doi.org/10.1007/s13367-014-0011-7.

5. Pan X, Tasdelen MA, Laun J, Junkers T, Yagci Y, Matyjaszewski K. Photomediated controlled radical polymerization. Prog Polym Sci. 2016;62:73–125. https://doi.org/10.1016/j.progpolymsci.2016.06.005.

6. Baharvandi HR, Alebooyeh M, Alizadeh M, Heydari MS, Kordani N, Khaksari P. The influences of particle–particle interaction and viscosity of carrier fluid on characteristics of silica and calcium carbonate suspensions-coated Twaron® composite. J Exp Nanosci. 2016;11:550–63. https://doi.org/10.1080/17458080.2015.1094190.

7. Baharvandi HR, Alebooyeh M, Alizadeh M, Khaksari P, Kordani N. Effect of silica weight fraction on rheological and quasi-static puncture characteristics of shear thickening fluid-treated Twaron® composite. J Ind Text. 2016;46(2):473–94. https://doi.org/10.1177/1528083715589750.

8. Lu Z, Jing X, Sun B, Gu B. Compressive behaviors of warp-knitted spacer fabrics impregnated with shear thickening fluid. Compos Sci Technol. 2013;88:184–9. https://doi.org/10.1016/j.compscitech.2013.09.004.

9. Gürgen S, Kuşhan MC. The stab resistance of fabrics impregnated with shear thickening fluids including various particle size of additives. Compos A Appl Sci Manuf. 2017;94:50–60. https://doi.org/10.1016/j.compositesa.2016.12.019.

10. Tan ZH, Zuo L, Li WH, Liu LS, Zhai PC. Dynamic response of symmetrical and asymmetrical sandwich plates with shear thickening fluid core subjected to penetration loading. Mater Des 2016;94:105–10. https://doi.org/10.1016/j.matdes.2016.01.036.

11. Hasan-nezhad H, Yazdani M, Jeddi M. High- and low-velocity impact experiments on treated STF/3D glass fabrics. Thin-Walled Struct. 2022;171:108720. https://doi.org/10.1016/j.tws.2021.108720.

12. Selver E. Tensile and flexural properties of glass and carbon fibre composites reinforced with silica nanoparticles and polyethylene glycol. J Ind Text. 2020;49:809–32. https://doi.org/10.1177/1528083719827368.

13. Pinto F, Meo M. Design and manufacturing of a novel shear thickening fluid composite (STFC) with enhanced out-of-plane properties and damage suppression. Appl Compos Mater. 2017;24:643–60. https://doi.org/10.1007/S10443-016-9532-1/FIGURES/15.

14. Silva SP, Sabino MA, Fernandes EM, Correlo VM, Boesel LF, Reis RL. Cork: properties, capabilities and applications. Int Mater Rev. 2005;50:345–65. https://doi.org/10.1179/174328005X41168.

15. Sergi C, Tirillò J, Sarasini F, Pozuelo EB, Saez SS, Burgstaller C. The potential of agglomerated cork for sandwich structures: a systematic investigation of physical, thermal, and mechanical properties. Polymers. 2019. https://doi.org/10.3390/polym11122118.

16. Varela MM, Fernandes FAO, Alves de Sousa RJ. Development of an eco-friendly head impact protection device. Appl Sci. 2020;10:2492. https://doi.org/10.3390/app10072492.

17. Gürgen S, de Sousa RJA. Rheological and deformation behavior of natural smart suspensions exhibiting shear thickening properties. Archiv Civ Mech Eng. 2020;20:110. https://doi.org/10.1007/s43452-020-00111-4.

18. Ferreira Serra G, Fernandes FAO, Alves de Sousa RJ, Noronha E, Ptak M. New hybrid cork-STF (Shear thickening fluid) polymeric composites to enhance head safety in micro-mobility accidents. Composite Struct. 2022;301:116138. https://doi.org/10.1016/j.compstruct.2022.116138.

19. Gürgen S, Fernandes FAO, de Sousa RJA, Kuşhan MC. Development of eco-friendly shock-absorbing cork composites enhanced by a non-newtonian fluid. Appl Compos Mater. 2021. https://doi.org/10.1007/s10443-020-09859-7.

20. Chavan N, Dhage A, Wale A, Thorave A, Rajdeo K, Kamble S, Ponrathnam S, Tambe S, Verma S. Novel shear thickening fluids possessing high shear rates using monodispersed silica nanoparticles and PEG. Polym Bull. 2023;80:13069–98. https://doi.org/10.1007/s00289-023-04696-7.

21. Haris A, Lee HP, Tay TE, Tan VBC. Shear thickening fluid impregnated ballistic fabric composites for shock wave mitigation. Int J Impact Eng. 2015;80:143–51. https://doi.org/10.1016/j.ijimpeng.2015.02.008.

22. Fahool M, Sabet AR. UV-visible assessment of hydrocluster formation and rheological behaviour in bimodal and mono-disperse shear thickening fluids. Rheol Acta. 2015;54:77–83. https://doi.org/10.1007/s00397-014-0821-z.

23. Hasanzadeh M, Mottaghitalab V, Rezaei M. Rheological and viscoelastic behavior of concentrated colloidal suspensions of silica nanoparticles: a response surface methodology approach. Adv Powder Technol. 2015;26:1570–7. https://doi.org/10.1016/j.apt.2015.08.011.

24. Xu Y, Chen X, Wang Y, Yuan Z. Stabbing resistance of body armour panels impregnated with shear thickening fluid. Compos Struct. 2017;163:465–73. https://doi.org/10.1016/j.compstruct.2016.12.056.

25. Yanen C, Solmaz MY, Aydoğmuş E, Arslanoğlu H. Effects of molecular weight of polyethylene glycol with size and ratio of fumed silica on rheological behavior of shear thickening fluid. Mater Chem Phys. 2024;312:128624. https://doi.org/10.1016/j.matchemphys.2023.128624.

26. Liu D-M. Particle packing and rheological property of highly-concentrated ceramic suspensions: φm determination and viscosity prediction. J Mater Sci. 2000;35:5503–7. https://doi.org/10.1023/A:1004885432221.

27. Liu X-Q, Bao R-Y, Wu X-J, Yang W, Xie B-H, Yang M-B. Temperature induced gelation transition of a fumed silica/PEG shear thickening fluid. RSC Adv. 2015;5:18367–74. https://doi.org/10.1039/C4RA16261G.

28. Bossis G, Brady JF. The rheology of Brownian suspensions. J Chem Phys. 1989;91:1866–74. https://doi.org/10.1063/1.457091.

29. Gürgen S, Kuşhan MC, Li W. The effect of carbide particle additives on rheology of shear thickening fluids. Korea-Aust Rheol J. 2016;28:121–8. https://doi.org/10.1007/s13367-016-0011-x.

30. Gürgen S, Li W, Kuşhan MC. The rheology of shear thickening fluids with various ceramic particle additives. Mater Des. 2016;104:312–9. https://doi.org/10.1016/j.matdes.2016.05.055.

31. Sheikhi MR, Gürgen S. Deceleration behavior of multi-layer cork composites intercalated with a non-Newtonian material.

Archiv Civ Mech Eng. 2022;23:2. https://doi.org/10.1007/s43452-022-00544-z.

32. Feng X, Li S, Wang Y, Wang Y, Liu J. Effects of different silica particles on quasi-static stab resistant properties of fabrics impregnated with shear thickening fluids. Mater Des. 2014;64:456–61. https://doi.org/10.1016/j.matdes.2014.06.060.

33. Chatterjee VA, Dey P, Verma SK, Bhattacharjee D, Biswas I, Neogi S. Probing the intensity of dilatancy of high performance shear-thickening fluids comprising silica in polyethylene glycol. Mater Res Express. 2019;6:075702. https://doi.org/10.1088/2053-1591/ab1185.

34. Singh M, Verma SK, Biswas I, Mehta R. Effect of addition of silicone oil on the rheology of fumed silica and polyethylene glycol shear thickening suspension. J Polym Eng. 2019;39:48–57. https://doi.org/10.1515/polyeng-2018-0054.

Publisher's Note Springer Nature remains neutral with regard to jurisdictional claims in published maps and institutional affiliations.

Authors and Affiliations

L. Oliveira[1] · G. F. Serra[1,2] · S. Gürgen[3] · R. M. Novais[4] · R. J. Alves de Sousa[1,2] · F. A. O. Fernandes[1,2]

✉ F. A. O. Fernandes
fabiofernandes@ua.pt

1 Centre for Mechanical Technology and Automation (TEMA), Department of Mechanical Engineering, University of Aveiro, Campus Universitário de Santiago, 3810-193 Aveiro, Portugal

2 LASI—Intelligent Systems Associate Laboratory, Guimarães, Portugal

3 Department of Aeronautical Engineering, Eskişehir Osmangazi University, Eskişehir, Turkey

4 Department of Materials and Ceramic Engineering, CICECO-Aveiro Institute of Materials, University of Aveiro, Campus Universitário de Santiago, 3810-193 Aveiro, Portugal